Effect of $E1$ excitations to the continuum: ^{6}He and ^{6}Li+^{209}Bi compared

N. Keeley,* J. M. Cook, K. W. Kemper, B. T. Roeder, and W. D. Weintraub
Department of Physics, The Florida State University, Tallahassee, Florida 32306-4350, USA

F. Maréchal
Institut de Recherches Subatomiques, BP28, F-67037 Strasbourg, Cedex 2, France

K. Rusek
Department of Nuclear Reactions, The Andrzej Sołtan Institute for Nuclear Studies, Hoża 69 00-681, Warsaw, Poland
(Received 3 July 2003; published 4 November 2003)

We compare existing elastic scattering data for ^{6}He+^{209}Bi with new ^{6}Li+^{209}Bi data at the same center of mass energies relative to their respective Coulomb barriers. Total reaction cross sections obtained from optical model fits to the ^{6}Li+^{209}Bi elastic scattering data confirm previous suggestions that the total reaction cross section for ^{6}He+^{209}Bi is much larger than that for the ^{6}Li+^{209}Bi system at similar energies relative to the Coulomb barrier. Continuum-discretized coupled channels calculations suggest that the enhanced reaction cross section for ^{6}He is due to the large $E1$ excitation strength to the continuum, absent in ^{6}Li. However, this conclusion is still tentative, as the calculations predict a large peak in the total α yield at forward angles which the currently available data are unable to confirm, due to their not extending to sufficiently small angles. New *precise* data for the elastic scattering and total α yield at forward angles for the ^{6}He+^{209}Bi system are required to confirm the contribution of $E1$ excitation to the continuum to the total reaction cross section.

DOI: 10.1103/PhysRevC.68.054601 PACS number(s): 21.60.Gx, 24.10.Eq, 24.10.Ht, 25.60.Bx

I. INTRODUCTION

In the $\alpha+d$ two-body cluster picture of ^{6}Li all electric dipole transition strengths are identically equal to zero, due to the recoil parameter β_1 equating to zero for this particular cluster-core combination in the expression for the electric dipole transition operator [1]:

$$\beta_1 = \frac{A_1Z_2 - A_2Z_1}{(A_1 + A_2)}, \tag{1}$$

with A_1, Z_1=4, 2 and A_2, Z_2=2, 1 for ^{6}Li. This lack of dipole strength in ^{6}Li makes a comparison with ^{6}He, which has a strong dipole excitation mode [2], particularly interesting as both nuclei are of similar size, the interaction nuclear radii derived from interaction cross section measurements [3] being 2.18±0.02 fm and 2.09±0.02 fm for ^{6}He and ^{6}Li, respectively, and both are weakly bound, the breakup threshold for $^6\mathrm{Li}\rightarrow\alpha+d$ being 1.47 MeV and that for $^6\mathrm{He}\rightarrow\alpha+2n$ 0.973 MeV.

Recent work comparing ^{6}Li and ^{6}He elastic scattering from a ^{208}Pb target [4] has shown that the effect of the strong electric dipole coupling to the continuum in ^{6}He is readily apparent in the measured angular distribution for ^{6}He+^{208}Pb elastic scattering at a ^{6}He laboratory energy of 29.6 MeV. Measurements of ^{6}He+^{209}Bi elastic scattering and total α yield plus fusion cross sections [5,6] indicate a large total reaction cross section persisting to energies below the nominal Coulomb barrier, in contrast to the measured total α yields for the ^{6}Li+^{208}Pb system at similar energies relative to the Coulomb barrier [7]. An important question, then, is whether this large total reaction cross section arises from the difference in binding energy between the two projectiles or from the electric dipole coupling to the continuum present in ^{6}He but absent in ^{6}Li.

In order to address this question, we present new ^{6}Li+^{209}Bi elastic scattering data, taken at similar center of mass energies relative to the Coulomb barrier to those of the previous ^{6}He+^{209}Bi results. New data were obtained to keep as many parameters as possible the same between the two systems under study. Total reaction cross sections for the ^{6}Li+^{209}Bi system extracted from optical model fits to the elastic scattering data are compared with those obtained for the ^{6}He+^{209}Bi system. The data for both systems are analyzed by means of continuum-discretized coupled channels (CDCC) calculations in order to elucidate the role of $E1$ excitation to the continuum and/or the lower breakup threshold of ^{6}He in producing the enhanced total reaction cross section for the ^{6}Li+^{209}Bi system.

A brief description of the experimental procedure for the ^{6}Li+^{209}Bi elastic scattering measurements is provided in Sec. II and the optical model fitting procedure is described in Sec. III. The CDCC calculations are described in Sec. IV and the results discussed in Sec. V. Section VI provides a summary of our conclusions.

II. EXPERIMENTAL PROCEDURE

In order to compensate for the increased charge of ^{6}Li compared to ^{6}He we carried out measurements of the ^{6}Li+^{209}Bi elastic scattering at the same value of $E_{\mathrm{c.m.}}-E_{\mathrm{b}}$ as for the previous ^{6}He+^{209}Bi measurements [5,6], where $E_{\mathrm{c.m.}}$ is the center of mass frame energy and E_{b} is the nominal Coulomb barrier energy. We used values of 31.5 MeV and

*Email address: keeley@nucmar.physics.fsu.edu

TABLE I. Best-fit optical model parameters for the ^{6}Li+^{209}Bi elastic scattering data. Potential depths are given in MeV and radius and diffuseness parameters in fm. Potential radii are given by $R_x = r_x \times 209^{1/3}$ fm. The Coulomb potential radius is r_c=1.9 fm.

$E(^6\text{Li})$	V	r_0	a_0	W	r_W	a_W	σ_R (mb)	χ^2/N
29.9	50.0	1.41	0.63	113.19	1.53	0.68	278	1.8
32.8	50.0	1.41	0.77	95.55	1.53	0.65	514	1.7

20.1 MeV for the ^{6}Li+^{209}Bi and ^{6}He+^{209}Bi Coulomb barriers, respectively.

A ^{6}Li beam was produced by a standard sputter ion source and accelerated to energies of 29.9 MeV and 32.8 MeV by the Florida State University FN tandem van de Graaf accelerator. Targets were 150 μg/cm^{2} ^{209}Bi on either a carbon or formvar backing. Three silicon surface barrier detector $\Delta E-E$ telescopes on movable arms were placed on one side of the beam to measure the elastic scattering angular distribution and a single monitor detector was placed on the opposite side of the beam at a fixed laboratory frame angle of 20° for normalization purposes (at these beam energies the ^{6}Li+^{209}Bi elastic scattering cross section at 20° is equal to the Rutherford scattering cross section).

Angle settings for the movable arms were chosen such that at least three points overlapped between settings to ensure reliable normalization. In the subsequent data reduction process points lying less than 1.0° apart were merged by taking an error-weighted mean. Overall normalization of the data was obtained by setting the most forward angle cross section data to be equal to the Rutherford scattering cross section.

III. OPTICAL MODEL ANALYSIS

An optical model analysis of the new ^{6}Li+^{209}Bi elastic scattering data was performed in order to extract total reaction cross sections σ_R to compare with those obtained for the ^{6}He+^{209}Bi system by Aguilera *et al.* [6]. The analysis was carried out using the code HIOPTIM [8]. The best-fit optical potential parameters, χ^2/point, and total reaction cross section values are given in Table I.

Both real and imaginary potentials were of standard Woods-Saxon form.

The ^{6}Li+^{209}Bi total reaction cross section is much smaller (by a factor of approximately 2−2.5) than that for ^{6}He+^{209}Bi, as inferred by Aguilera *et al.* [6] from ^{6}Li+^{208}Pb cross sections at similar energies. It is tempting to ascribe the large difference in total reaction cross sections between the ^{6}He+^{209}Bi and ^{6}Li+^{209}Bi systems as due to the difference in the breakup threshold between ^{6}He and ^{6}Li, as was done for ^{6}Li and ^{7}Li in the case of the ^{6}Li+^{208}Pb and ^{7}Li+^{208}Pb systems [9]. However, the difference in breakup thresholds between ^{6}He and ^{6}Li is approximately half that between ^{6}Li and ^{7}Li. The strong dipole coupling strength in ^{6}He, much stronger than that in ^{7}Li, could also play a role. In order to further probe this question we performed a series of CDCC calculations, described in the following section.

IV. THE CDCC CALCULATIONS

We carried out CDCC calculations for both ^{6}Li+^{209}Bi and ^{6}He+^{209}Bi using the two-body cluster-folding model formulation of Buck and Pilt [1]. While the ^{6}Li nucleus is well described as an $\alpha+d$ two-body cluster, ^{6}He is considered to be a three-body $\alpha+n+n$ object. However, the three-body wave function for the ^{6}He ground state has a dineutron (^{2}n) component that dominates the tail [10], resulting in an $\alpha+^{2}n$ cluster structure. As low-energy scattering from a heavy target is only sensitive to the tail of the wave function, this model is expected to be adequate to describe the breakup effects in this case. In both cases, we ignored the 9/2 ground state spin of ^{209}Bi, setting this to 0 in order to obtain a tractable calculation. This procedure does not affect the cross sections resulting from the calculations. The CDCC formalism is described in detail by Sakuragi *et al.* [11].

The ^{6}Li+^{209}Bi calculations were similar to those of Keeley *et al.* [12]. The $\alpha+d$ continuum model space was limited to relative orbital angular momentum values $L=0,1,2$ and was discretized into a series of bins with respect to the momentum $\hbar k$ of the relative $\alpha+d$ motion. The bins were limited to $0.0 \leqslant k \leqslant 0.75$ fm^{-1} with $\Delta k=0.25$ fm^{-1}. The $\alpha+d$ wave functions were averaged over the bin width and were not normalized to unity, the radius limiting their range being set to 80 fm. This binning scheme was suitably modified for the $L=2$ continuum in order to avoid double counting due to the presence of the three $L=2$ resonant states. These were treated as bins of width ΔE=0.1, 2.0, and 3.0 MeV for the 2.18-MeV 3^+, 4.31-MeV 2^+, and 5.7-MeV 1^+ resonances, respectively. The $\alpha+^{209}$Bi and $d+^{209}$Bi optical potentials used as input to the cluster-folding model were calculated using the global potentials of Avrigeanu *et al.* [13] and Perey and Perey [14], respectively, renormalized by a factor of 0.8 for both real and imaginary parts. All partial waves up to $\ell=200$ were included in the calculations.

For the ^{6}He+^{209}Bi calculations we adopted the procedure of Rusek *et al.* [4]. The $\alpha+^{2}n$ continuum was limited to relative orbital angular momentum values $L=0,1,2$ and discretized into bins in relative $\alpha+^{2}n$ momentum space limited to $0.0 \leqslant k \leqslant 0.6$ fm^{-1}, with $\Delta k=0.1$ fm^{-1}. The wave functions were not normalized to unity and the radius limiting their range was set to 300 fm. The binning scheme for the $L=2$ continuum was modified in order to avoid double counting due to the presence of the 1.8-MeV 2^+ resonance, which was treated as a bin of width ΔE=0.3 MeV. The finer binning scheme and larger limiting radius for ^{6}He compared to ^{6}Li were necessary due to the long-range strong $E1$ Coulomb breakup component in ^{6}He. The $\alpha+^{209}$Bi and $^{2}n+^{209}$Bi optical potentials needed for the cluster-folding model were again taken from the global potentials of Avrigeanu *et al.* [13] and Perey and Perey [14], the real and imaginary parts being renormalized by factors of 0.8 and 1.0, respectively. All partial waves up to $\ell=175$ or 250 were included in the calculations for ^{6}He bombarding energies of 19.0 MeV and 22.5 MeV, respectively.

The results of these calculations are given in Figs. 1 and 2.

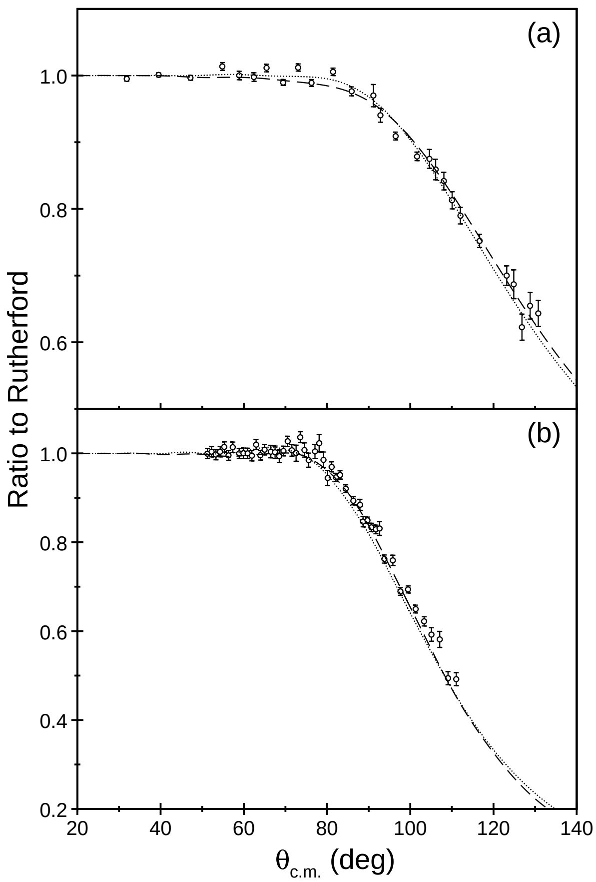

FIG. 1. CDCC calculations for ^{6}Li+^{209}Bi at ^{6}Li bombarding energies of 29.9 MeV (a) and 32.8 MeV (b). The dashed curves indicate the results of the full calculations, while the dotted curves indicate the results of calculations that include only nuclear coupling to the continuum. Note the linear cross section scale.

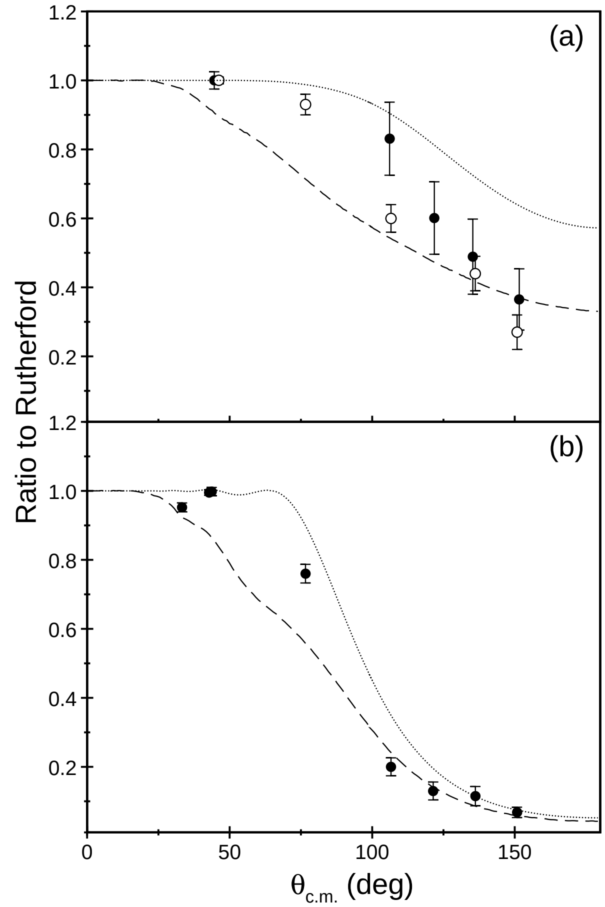

FIG. 2. CDCC calculations for ^{6}He+^{209}Bi at ^{6}He bombarding energies of 19.0 MeV (a) and 22.5 MeV (b). The dashed curves indicate the results of the full calculations, while the dotted curves indicate the results of calculations that include only nuclear coupling to the continuum. Note the linear cross section scale.

As can be seen, while we obtain a very good description of the ^{6}Li+^{209}Bi elastic scattering data, the ^{6}He+^{209}Bi data are rather poorly described, unlike the 29.6-MeV ^{6}He +^{208}Pb elastic scattering data which were well described by the α+^{2}n model of ^{6}He [4]. The calculated ^{6}He+^{209}Bi elastic scattering angular distributions were found to be relatively insensitive to the choice of α+^{209}Bi and ^{2}n+^{209}Bi optical potentials and consistently fell below the data in the angular range 50°–100°.

One may note that the 19-MeV ^{6}He+^{209}Bi data have been normalized to be equal to the Rutherford scattering cross section at the most forward angle point measured. A renormalization of the data by a factor of ~0.9 would produce a good match to our calculated angular distribution. However, with the currently available data there is no independent justification for such a renormalization procedure, and further data at smaller scattering angles are required to settle this point. The situation for the ~22-MeV ^{6}He data is less clear, as our calculation matches all but two of the measured points. Again, further data will be necessary to definitively decide whether or not the α+^{2}n model is adequate to describe the ^{6}He+^{209}Bi elastic scattering.

An important difference between the results of the calculations for the ^{6}Li+^{209}Bi and the ^{6}He+^{209}Bi systems is in the influence of Coulomb excitation to the continuum on the elastic scattering. Figures 1 and 2 show the predicted elastic scattering angular distributions for calculations that include only nuclear excitations to the continuum as dotted curves (only the diagonal Coulomb terms are retained in these calculations). While it is readily apparent that the omission of the Coulomb excitation has little effect on the predicted ^{6}Li +^{200}Bi elastic scattering angular distributions, as noted previously for the ^{6}Li+^{208}Pb system [15], Coulomb excitation to the continuum has a very large effect on the predicted elastic scattering angular distributions for the ^{6}He+^{209}Bi system. This is due to the strong *E*1 Coulomb coupling in ^{6}He, absent in ^{6}Li, as shown for the ^{6}He+^{208}Pb system by Rusek *et al.* [4].

In Fig. 3 we show the predicted total reaction cross sections σ_{R} of our ^{6}Li+^{209}Bi and ^{6}He+^{209}Bi CDCC calculations, denoted by the filled circles and filled squares, respectively.

While the ^{6}Li+^{209}Bi CDCC calculations give total reaction cross sections that agree well with those obtained from the optical model fits to the elastic scattering data, the ^{6}He +^{209}Bi CDCC calculations give total reaction cross sections about three times larger than the sum of the measured total α yield and fusion cross sections or the total reaction cross

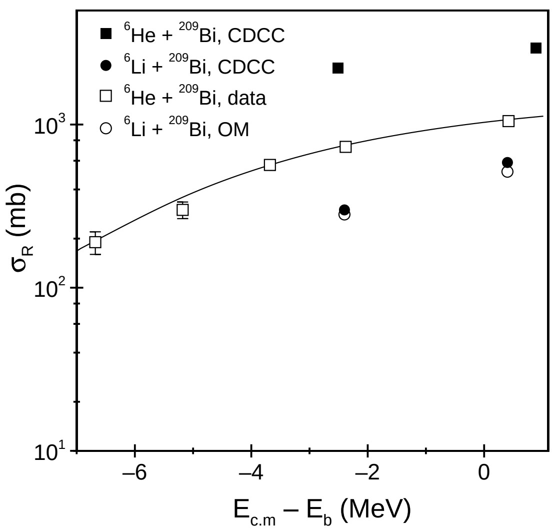

FIG. 3. Predicted ^{6}Li+^{209}Bi (filled circles) and ^{6}He+^{209}Bi (filled squares) total reaction cross sections from the CDCC calculations. Also shown are the ^{6}Li+^{209}Bi total reaction cross sections obtained from the optical model fits to the data (open circles) and the measured total α yield plus fusion cross sections of Aguilera *et al.* [6] (open squares). The solid line denotes the total reaction cross sections obtained from the optical model fit of Aguilera *et al.*

section obtained from the optical model fit of Aguilera *et al.* [6]. This overprediction of the ^{6}He+^{209}Bi total reaction cross section is related to the underprediction of the elastic scattering angular distributions at intermediate angles: the CDCC calculations have too much absorption compared to the data.

It should be noted that the ^{6}He+^{209}Bi CDCC calculations were carried out at incident ^{6}He energies of 19.0 and 22.5 MeV. In this choice of energy we have followed the original publication of Aguilera *et al.* [5] which quotes these laboratory frame energies. There is a slight discrepancy between these values and the center of mass frame values quoted in the later paper of Aguilera *et al.* [6] which correspond to laboratory frame energies of 19.1 and 22.0 MeV, respectively. In plotting the measured total α yield plus fusion cross sections we have used the center of mass frame energies of Ref. [6]. We mention this slight discrepancy (which may be ascribed to uncertainties in the exact energy of the ^{6}He radioactive beam) as the method of presentation as a function of $E_{\text{c.m.}}-E_{\text{b}}$ tends to exaggerate it.

In Figs. 4 and 5 we show the predicted $^6\text{Li}\rightarrow\alpha+d$ and $^6\text{He}\rightarrow\alpha+{}^2n$ breakup angular distributions.

The dashed curves indicate the results of the full calculations while the dotted curves denote the results of calculations that include only nuclear excitation to the continuum (plus the diagonal Coulomb terms). As might be expected, Coulomb breakup is important for both systems.

Also shown in Fig. 5, as the solid points, are the measured total α yield angular distributions of Aguilera *et al.* [5]. It is immediately apparent that while our calculations underestimate the measured yield at backward angles they predict a large peak at forward angles. The data of Aguilera *et al.* do not extend sufficiently far forward in angle to observe such a peak, if present, although for the data obtained with an incident ^{6}He energy of 22.5 MeV our calculation is significantly above the data point at an angle of ~45°. Evidently, further measurements of the total α yield at angles forward of ~50° are required to settle this point.

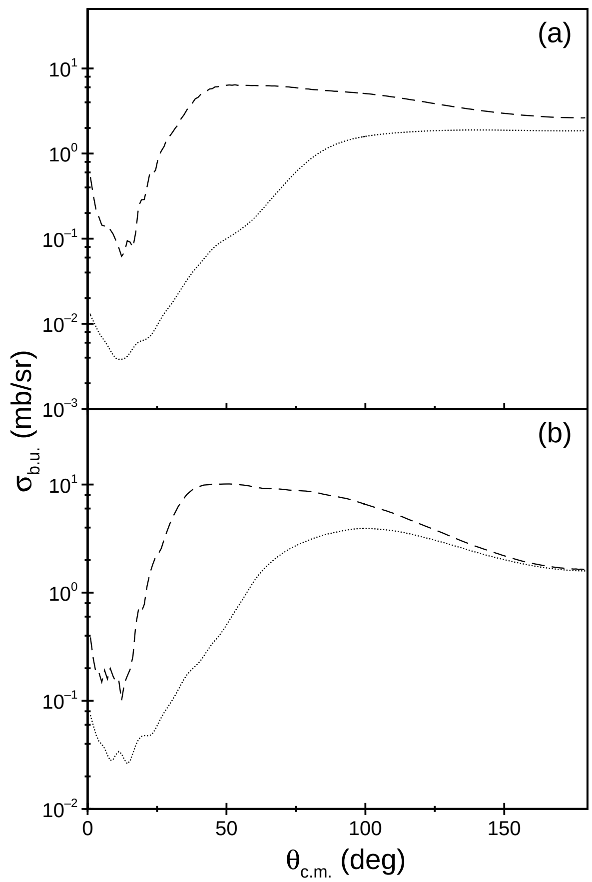

FIG. 4. Predicted $^6\text{Li}\rightarrow\alpha+d$ breakup angular distributions for ^{6}Li+^{209}Bi at ^{6}Li bombarding energies of 29.9 MeV (a) and 32.8 MeV (b). The dashed curves indicate the results of the full calculations, while the dotted curves indicate the results of calculations that include only nuclear coupling to the continuum.

It should also be pointed out that although the total α yield angular distributions of Aguilera *et al.* [5] are given in the center of mass frame, such a transformation is not in principle possible for an inclusive measurement. If the α particle only is detected one has no *a priori* knowledge of the mechanism that produced it, hence an unambiguous transformation from the laboratory to the center of mass frame is not possible. However, this should not be a major issue for the ^{6}He+^{209}Bi system due to the large difference in mass between the target and the projectile.

We also performed CDCC calculations for ^{6}Li+^{209}Bi where the $\alpha+d$ breakup threshold was set equal to the α +2n breakup threshold of ^{6}He (all other parameters being left unchanged) in order to test the effect of the breakup threshold on the predicted elastic scattering and breakup cross sections. The results are plotted in Figs. 6 and 7 as the dot-dashed curves.

It will be noted that the effect of lowering the breakup threshold on the elastic scattering is small, while the effect on the predicted breakup is to increase the total breakup cross section by a factor of ~2. By contrast, the predicted

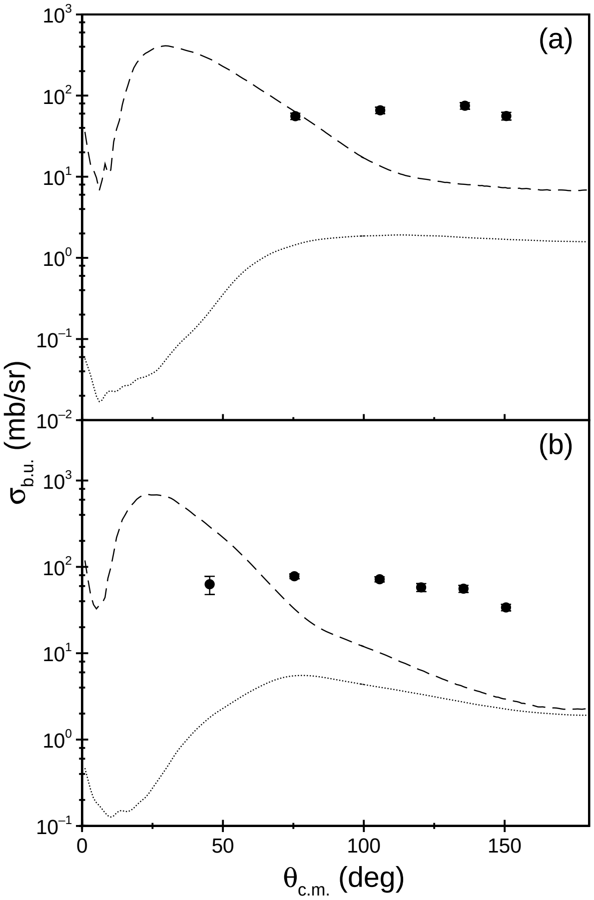

FIG. 5. Predicted ^{6}He→α+^{2}n breakup angular distributions for ^{6}He+^{209}Bi at ^{6}He bombarding energies of 19.0 MeV (a) and 22.5 MeV (b). The dashed curves indicate the results of the full calculations, while the dotted curves indicate the results of calculations that include only nuclear coupling to the continuum. The solid points denote the total α yield angular distributions of Aguilera *et al.* [5].

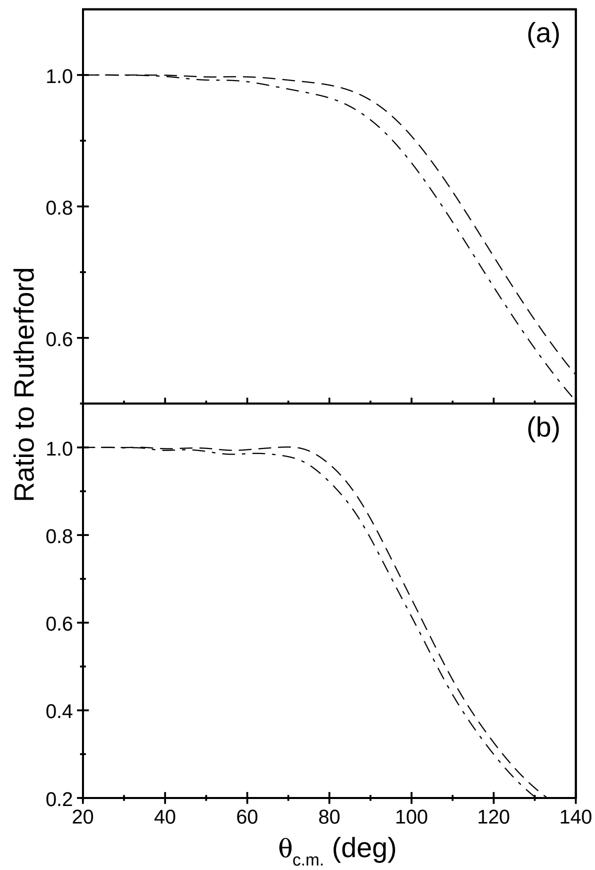

FIG. 6. CDCC calculations for ^{6}Li+^{209}Bi at ^{6}Li bombarding energies of 29.9 MeV (a) and 32.8 MeV (b). The dashed curves indicate the results of the physical calculations, while the dot-dashed curves indicate the results of calculations where the α+d threshold was set equal to the α+2n threshold of ^{6}He. The data points have been omitted for clarity.

^{6}He→α+^{2}n breakup cross section is ~20 times larger than the predicted ^{6}Li→α+d breakup cross section using the physical breakup threshold.

V. DISCUSSION

A comparison of new ^{6}Li+^{209}Bi data with existing results for ^{6}He+^{209}Bi [5,6] has confirmed that the total reaction cross section for the ^{6}Li+^{209}Bi system is much smaller than that for the ^{6}He+^{209}Bi system at similar energies relative to their respective Coulomb barriers. However, while CDCC calculations are able to provide a good description of the ^{6}Li+^{209}Bi elastic scattering angular distributions and total reaction cross sections, similar calculations for the ^{6}He+^{209}Bi system are not. In particular, the calculations fall below the measured elastic scattering angular distributions at intermediate scattering angles and yield total reaction cross sections approximately a factor of 3 times larger than the sum of the measured total α yield plus fusion cross sections or the total reaction cross section extracted from an optical model fit to the data [6].

A comparison of the calculated total breakup cross section angular distributions for the ^{6}He→α+^{2}n process with the measured total α yield angular distributions of Aguilera *et al.* [5] showed that while the calculations underpredict the data at backward angles, they predict a large peak at forward angles. The current data do not extend far enough forward in angle to determine whether such a peak is actually present. However, for an incident ^{6}He energy of 22.5 MeV the CDCC calculation considerably overpredicts the total α yield differential cross section at ~45°, the smallest angle measured, suggesting that the coupling strength to the ^{6}He+2n continuum may be too strong in our two-body α+^{2}n model.

To set against the suggestion that the α+^{2}n model produces coupling to the continuum that is too strong, we have the calculations of Rusek *et al.* [4] that well reproduce 29.6 MeV ^{6}He+^{208}Pb elastic scattering data. In fact, these data suggest that the continuum coupling strength may actually be somewhat too small, as the predicted elastic scattering angular distribution is slightly higher than the data in the intermediate angle range. Thus, the available elastic scattering and reaction data for ^{6}He interacting with a heavy target appear to lead to conflicting conclusions concerning the α+^{2}n model of ^{6}He.

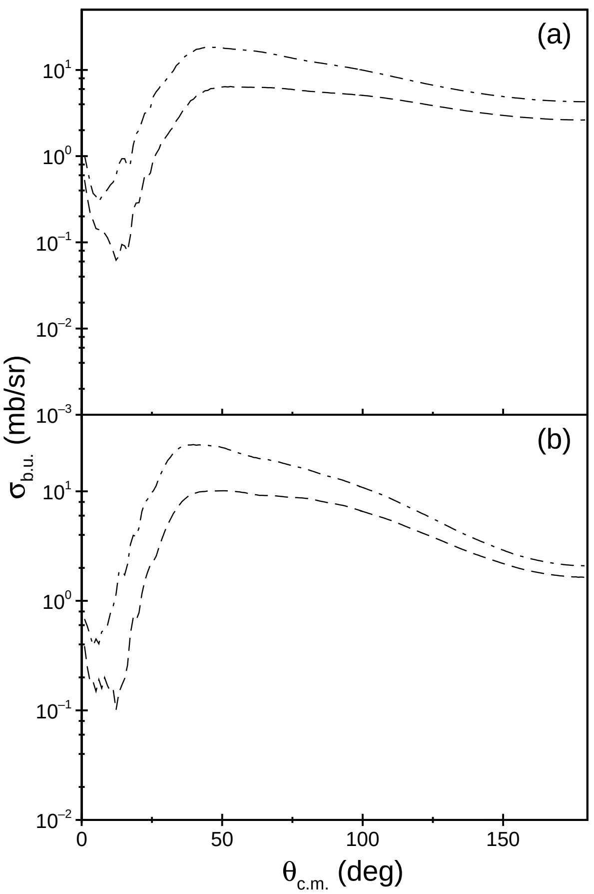

FIG. 7. Predicted ^{6}Li$\rightarrow\alpha+d$ breakup angular distributions for ^{6}Li+^{209}Bi at ^{6}Li bombarding energies of 29.9 MeV (a) and 32.8 MeV (b). The dashed curves indicate the results of the physical calculations, while the dot-dashed curves indicate the results of calculations where the $\alpha+d$ threshold was set equal to the $\alpha+2n$ threshold of ^{6}He.

As the main continuum coupling influence on the elastic scattering is the dipole Coulomb breakup [4], we may also compare our model $E1$ coupling strength against the energy weighted sum rule (EWSR) as an additional check. In the present $\alpha+^2n$ model of ^{6}He the dipole coupling strength up to a ^{6}He excitation energy E^* of 6.62 MeV (the upper limit of the top-most continuum bin) exhausts 23.7% of the Thomas-Reiche-Kuhn (TRK) EWSR, given by [16]

$$S(E1)_{\rm TRK} = \sum E^* B(E1)\uparrow\ = 14.8\frac{NZ}{A}\text{MeV } e^2 \text{ fm}^2, \quad (2)$$

and 95% of the cluster EWSR, given by [17]

$$S(E1)_{\rm cluster} = 14.8\frac{(Z_1A_2 - Z_2A_1)^2}{AA_1A_2}\text{MeV } e^2 \text{ fm}^2, \quad (3)$$

where the nucleus of mass and charge A,Z is formed of "core" and "valence" clusters of mass and charge A_1,Z_1 and A_2,Z_2, respectively. These results compare quite well with the experimental values of Aumann *et al.* [2] of (9.6 ± 2.0)% and (38.5 ± 8.1)% of the TRK and cluster EWSR integrating the measured $E1$ strength function up to $E^*=5$ MeV and (32.4 ± 6.6)% and (129.8 ± 26.4)% of the TRK and cluster EWSR integrating the measured $E1$ strength distribution function up to $E^*=10$ MeV. Thus, we may conclude that the $E1$ coupling strength in the $\alpha+^2n$ model of ^{6}He is not unreasonably large.

The discrepancy between the calculated ^{6}He$\rightarrow\alpha+^2n$ breakup and measured total α yield angular distributions at backward angles is similar to that observed in the ^{6}Li+^{208}Pb system [18]. Signorini *et al.* [18] also obtained exclusive $\alpha+d$ coincidence data which were well described by CDCC calculations similar to those described here. Thus, the direct breakup component of the total α yield for the ^{6}Li+^{208}Pb system is well understood, the backward angle α yield being conjectured to be mainly due to partial fusion and/or transfer processes yielding an α particle.

Similar processes may be conjectured to be responsible for this part of the observed total α yield angular distribution for the ^{6}He+^{209}Bi system. Calculations of ^2n transfer to unbound states in the ^{209}Bi+^2n continuum of ^{211}Bi reported in Aguilera *et al.* [5] support this conjecture. Other processes, such as single neutron transfer to states in ^{210}Bi which leave an unbound ^{5}He as projectilelike residue, may also contribute, although test distorted-wave Born approximation calculations suggest that any such transfers must be to states close to the ^{209}Bi+n threshold in ^{210}Bi if they are to make a significant contribution to the total α yield.

Test ^{6}Li+^{209}Bi CDCC calculations where the $\alpha+d$ threshold was set equal to the $\alpha+2n$ threshold of ^{6}He indicate the crucial role played by the strong $E1$ coupling in ^{6}He in producing the much larger breakup cross section for ^{6}He compared to ^{6}Li. As Fig. 7 shows, merely reducing the breakup threshold of ^{6}Li to match that of ^{6}He does not increase the predicted ^{6}Li$\rightarrow\alpha+d$ breakup cross section sufficiently to match that of the ^{6}He$\rightarrow\alpha+^2n$ breakup at a similar energy with respect to the appropriate Coulomb barrier. A comparison of Fig. 5 with Fig. 7 shows that the forward angle peak in the predicted ^{6}He$\rightarrow\alpha+^2n$ breakup angular distributions may be ascribed to the $E1$ Coulomb coupling to the continuum—such a peak is not present in the predicted ^{6}Li$\rightarrow\alpha+d$ breakup angular distributions of the test calculations with the lowered breakup threshold.

Thus, our calculations lead us to conclude that the strong $E1$ Coulomb coupling to the continuum in ^{6}He not only has the dominant influence on the elastic scattering of ^{6}He by a heavy target, as was found by Rusek *et al.* [4], but is also the main cause of the much larger total reaction cross sections observed by Aguilera *et al.* [5,6] for ^{6}He+^{209}Bi compared to those reported here for ^{6}Li+^{209}Bi at similar energies with respect to the relevant Coulomb barrier.

However, this conclusion must be regarded as tentative until new *precise* elastic scattering data for ^{6}He from a heavy target (either ^{208}Pb or ^{209}Bi) at energies comparable to the existing data of Aguilera *et al.* [5,6], combined with forward angle total α yield data, have been obtained. These new data are required in order to confirm (or refute) the large forward angle peak in the ^{6}He$\rightarrow\alpha+^2n$ breakup angular distribution and the corresponding larger total reaction cross section predicted by the $\alpha+^2n$ model of ^{6}He.

VI. SUMMARY

In this work we have compared data for ^{6}He+^{209}Bi and ^{6}Li+^{209}Bi at similar center of mass energies relative to their respective Coulomb barriers to confirm the previously suggested enhanced total reaction cross section for ^{6}He compared to ^{6}Li, and to establish whether this enhancement is due to the lower breakup threshold of ^{6}He or to the $E1$ coupling to the continuum, present in ^{6}He but absent in ^{6}Li. New ^{6}Li+^{209}Bi elastic scattering data were obtained at ^{6}Li bombarding energies of 29.9 and 32.8 MeV. Total reaction cross sections extracted from optical model fits to these data confirm the earlier conclusion of Aguilera *et al.* [6] that the total reaction cross section for the ^{6}He+^{209}Bi system is considerably enhanced, being a factor of ≈2–2.5 times larger than the corresponding ^{6}Li+^{209}Bi cross section.

CDCC calculations were carried out for both ^{6}Li and ^{6}He+^{209}Bi in order to establish whether the enhanced ^{6}He total reaction cross section could be ascribed to its lower breakup threshold or to the strong $E1$ excitation to the continuum in ^{6}He, absent in ^{6}Li. These calculations suggest that the enhanced ^{6}He total reaction cross section is due to the strong $E1$ coupling to the continuum in ^{6}He rather than the smaller breakup threshold energy. However, this conclusion is still rather tentative as the CDCC calculations for ^{6}He +^{209}Bi, in contrast to those for ^{6}Li+^{209}Bi, were unable to describe the ^{6}He+^{209}Bi elastic scattering angular distributions at intermediate angles. Furthermore, the calculations predict a strong forward angle peak in the $^{6}\text{He}\rightarrow\alpha+{}^{2}n$ breakup angular distributions that the currently available total α yield data are unable to confirm as they do not extend sufficiently far forward in angle.

Comparisons of our ^{6}He model $E1$ strength with the Thomas-Reiche-Kuhn and cluster energy weighted sum rules indicate that they are physically reasonable. Therefore, we suggest that new *precise* ^{6}He+^{209}Bi elastic scattering data, together with measurements of the total α yield at forward angles, are required in order to confirm our conclusions regarding the importance of the $E1$ coupling to the continuum in ^{6}He in producing the enhanced total reaction cross section. Indeed, our calculations suggest that this enhancement over the total reaction cross section for ^{6}Li+^{209}Bi at similar energies relative to the Coulomb barrier may be even greater than the currently available data indicate.

ACKNOWLEDGMENTS

The authors would like to thank Professor J. J. Kolata for providing the ^{6}He+^{209}Bi data in tabular form. This work was supported by the U.S. National Science Foundation, the U.S. Department of Energy, the State of Florida and NATO, Grant No. PST.CLG.978953.

[1] B. Buck and A. A. Pilt, Nucl. Phys. **A280**, 133 (1977).
[2] T. Aumann *et al.*, Phys. Rev. C **59**, 1252 (1999).
[3] I. Tanihata, H. Hamagaki, O. Hashimoto, Y. Shida, N. Yoshikawa, K. Sugimoto, O. Yamakawa, T. Kobayashi, and N. Takahashi, Phys. Rev. Lett. **55**, 2676 (1995).
[4] K. Rusek, N. Keeley, K. W. Kemper, and R. Raabe, Phys. Rev. C **67**, 041604 (R) (2003).
[5] E. F. Aguilera *et al.*, Phys. Rev. Lett. **84**, 5058 (2000).
[6] E. F. Aguilera *et al.*, Phys. Rev. C **63**, 061603(R) (2001).
[7] R. Ost, E. Speth, K. O. Pfeiffer, and K. Bethge, Phys. Rev. C **5**, 1835 (1972).
[8] N. M. Clarke (unpublished).
[9] G. R. Kelly *et al.*, Phys. Rev. C **63**, 024601 (2001).
[10] M. V. Zhukov, B. V. Danilin, D. V. Fedorov, J. M. Bang, I. J. Thompson, and J. S. Vaagen, Phys. Rep. **231**, 151 (1993).
[11] Y. Sakuragi, M. Yahiro, and M. Kamimura, Prog. Theor. Phys. Suppl. **89**, 136 (1986).
[12] N. Keeley *et al.*, Phys. Rev. C **67**, 044604 (2003).
[13] V. Avrigeanu, P. E. Hodgson, and M. Avrigeanu, Phys. Rev. C **49**, 2136 (1994).
[14] C. M. Perey and F. G. Perey, Phys. Rev. **132**, 755 (1963).
[15] N. Keeley and K. Rusek, Phys. Lett. B **375**, 9 (1996).
[16] A. Bohr and B. R. Mottleson, *Nuclear Structure* (Benjamin, Reading, MA, 1975), Vol. II.
[17] Y. Alhassid, M. Gai, and G. F. Bertsch, Phys. Rev. Lett. **49**, 1482 (1982).
[18] C. Signorini *et al.*, Phys. Rev. C **67**, 044607 (2003).